Chapter 7

APPENDICES

Appendix A

ORBIT CONTROL OF BEAM SEPARATION AND CROSSING ANGLE AT AN INTERACTION POINT

An algorithm used to provide simultaneous control of the transverse separation and crossing angle of colliding beams at an interaction point is presented.

Controlling both the beam separation and crossing angle at an interaction point s_P requires a closed orbit distortion using four separators; two on each side of the interaction region. A four-bump algorithm specifies the angular deflections, $\Delta\theta_i$, applied to the separators to produce a closed orbit deflection of a specified orbit displacement, x_p, and specified phase, $x_p^{'}$, at an interaction point. The four-bump is localized in that it produces an orbit distortion only in the region bounded by the first and last separator bump elements.

A four-bump is necessary because of the number of constraints and variables in the bump calculation. A local three-bump has three variables ($\Delta\theta$'s of the three-bump elements) and three constraints. One of the constraints is the magnitude of the bump at a given location and the other two constraints ensure that the bump is local; the outgoing position and phase at the two endpoints of the bump are constrained to zero. It is of interest to constrain both the separation and crossing angle at an interaction point s_P, along with keeping the bump local. Thus a second three-bump is needed to provide the additional constraint. The four-bump algorithm results from the addition of two localized three-bumps.

Consider the schematic of Figure A.1. Angular deflections representing two three-bumps (dashed and dotted lines) are added to create a four-bump (solid line). The effect an angular deflection of magnitude $\Delta\theta_0$ at s_0 has on a particle's orbit at s_1 is found using Equation 2.9, which is reproduced here for convenience:

$$x(s) = A\sqrt{\beta(s)}\sin(\psi(s) + \delta). \tag{A.1}$$

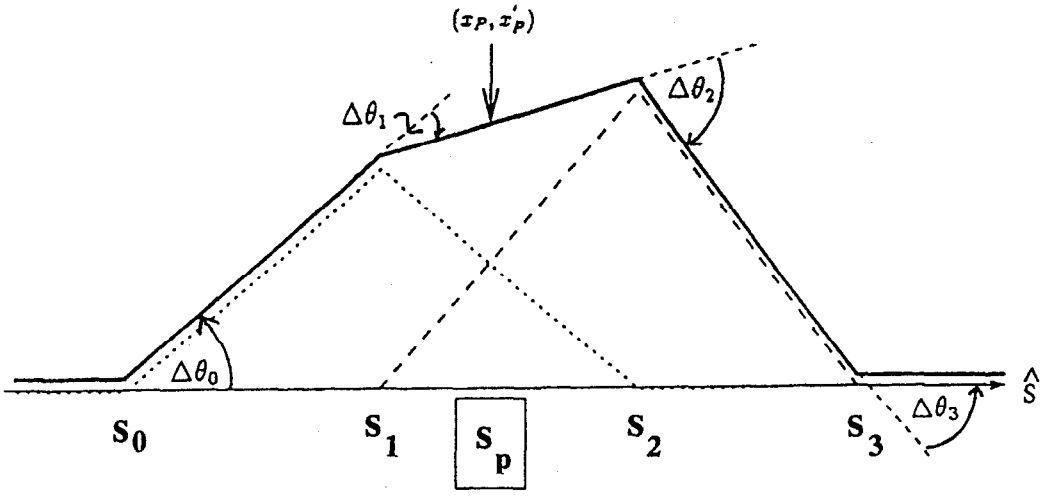

Figure A.1: Schematic of a four-bump which controls the position and phase at point s_P. The four-bump (solid line) is the result of the addition of two three-bumps (dotted and dashed lines). Angular deflections occur at longitudinal locations s_0,s_1,s_2 and s_3.

The constants A and δ are determined from initial conditions. Let $x_0 = 0$ at a location in which $\psi = 0$ and let $x_0' = \Delta\theta_0$ at that point. The solutions for the initial conditions are then found to be $\delta = 0$ and $A = \sqrt{\beta_0}\ \Delta\theta_0$. An orbit displacement x_1 at s_1 due to an angular deflection at s_0 is thus given by

$$x_1 = \Delta\theta_0\sqrt{\beta_1\beta_0}\sin\Delta\psi_{10}, \tag{A.2}$$

where $\Delta\psi_{10} = \psi_1 - \psi_0$ is the phase advance from s_0 to s_1. The lattice functions β_0 and β_1 are the beta functions at s_0 and s_1, respectively. The derivative of x_1 with respect to s gives x_1' in terms of $\Delta\theta_0$ as

$$x_1' = \Delta\theta_0\sqrt{\frac{\beta_0}{\beta_1}}\left[\cos\Delta\psi_{10} - \alpha_1\sin\Delta\psi_{10}\right]. \tag{A.3}$$

Both x_1 and x_1' depend on $\Delta\theta_0$ and on the lattice functions at s_0 and s_1. It is assumed that the lattice functions are known. As a result, the above expressions may be rewritten as

$$\begin{aligned} x_1 &= A\ \Delta\theta_0 \\ x_1' &= B\ \Delta\theta_0 \end{aligned} \tag{A.4}$$

where A and B are constants expressed in terms of lattice functions in Equations A.2 and A.3, respectively.

From Chapter 2 (Equation 2.13), a particle's traversal in one plane from s_P to s_1 is described by

$$\begin{pmatrix} x_1 \\ x_1' \end{pmatrix} = M_{P\to 1} \begin{pmatrix} x_P \\ x_P' \end{pmatrix}. \tag{A.5}$$

The elements of the transfer matrix depend entirely on the lattice functions at s_P and s_1. The orbit displacement and phase at s_1 is thus expressed in terms of the orbit displacement and phase at s_P multiplied by the constant matrix elements of $M_{P\to 1}$:

$$\begin{aligned} x_1 &= [(m_{11})_{P\to 1}]\, x_P + [(m_{12})_{P\to 1}]\, x_P' \\ x_1' &= [(m_{21})_{P\to 1}]\, x_P + [(m_{22})_{P\to 1}]\, x_P', \end{aligned} \tag{A.6}$$

where $(m_{ij})_{P\to 1}$ is the matrix element in the ith row and jth column of $M_{P\to 1}$. Solving for $\Delta\theta_0$ in terms of x_p and x_p' using Equations A.4 and A.6 yields two equations which must be simultaneously satisfied:

$$\begin{aligned} \Delta\theta_0 &= \frac{x_1}{A} = \frac{[(m_{11})_{P\to 1}]\, x_P + [(m_{12})_{P\to 1}]\, x_P'}{A} \\ \Delta\theta_0 &= \frac{x_1'}{B} = \frac{[(m_{21})_{P\to 1}]\, x_P + [(m_{22})_{P\to 1}]\, x_P'}{B}. \end{aligned} \tag{A.7}$$

If x_P is specified as a constraint, the two equations yield solutions for x_P' and x_1. A phase contribution at an interaction point, therefore, is introduced once an orbit displacement is specified. Similarly, specifying a particle's phase will introduce an orbit displacement. Once x_1 is known, the angular deflections for a localized three bump at s_0, s_1 and s_2 are found using the familiar three-bump algorithm.[9] The additional phase contribution which is introduced at the interaction point must then be cancelled by subtracting a second three-bump constrained to the same phase.

The angular deflections for the first three-bump at s_0,s_1 and s_2 are calculated using a local three-bump algorithm:[9]

$$\begin{aligned} \Delta\theta_{0a} &= \frac{x_{1a}}{\sqrt{\beta_0\beta_1}\sin(\psi_1-\psi_0)}, \\ \Delta\theta_{1a} &= \Delta\theta_{0a}\sqrt{\frac{\beta_0}{\beta_1}}\frac{\sin(\psi_2-\psi_0)}{\sin(\psi_2-\psi_1)}, \\ \Delta\theta_{2a} &= \Delta\theta_{0a}\sqrt{\frac{\beta_0}{\beta_2}}\frac{\sin(\psi_1-\psi_0)}{\sin(\psi_2-\psi_1)}. \end{aligned} \tag{A.8}$$

Note that $x_{1a} \equiv x_1$ in Equation A.6 above. The index a is added to the subscript of x_1 and $\Delta\theta_i$ in order to make a distinction between the two three-bump calculations.

Similarly, the angular deflections due to a second three-bump at s_1, s_2 and s_3 are calculated as follows. An angular deflection at s_1, $\Delta\theta_{1b}$, translates into an orbit displacement at s_2 of magnitude

$$x_{2b} = \Delta\theta_{1b}\sqrt{\beta_2\beta_1}\sin\Delta\psi_{21}. \tag{A.9}$$

The subscript b designates the second three bump. In terms of x_P and x'_P, the orbit displacement and phase at s_2 is given by

$$\begin{aligned} x_{2b} &= [(m_{11})_{P\to 2}]\, x_P + [(m_{12})_{P\to 2}]\, x'_P, \\ x'_{2b} &= [(m_{21})_{P\to 2}]\, x_P + [(m_{22})_{P\to 2}]\, x'_P. \end{aligned} \tag{A.10}$$

The angular deflections for the second three bump are given by

$$\begin{aligned} \Delta\theta_{1b} &= \frac{x_{2b}}{\sqrt{\beta_1\beta_2}\sin(\psi_2-\psi_1)}, \\ \Delta\theta_{2b} &= \Delta\theta_{1b}\sqrt{\frac{\beta_1}{\beta_2}}\frac{\sin(\psi_3-\psi_1)}{\sin(\psi_3-\psi_2)}, \\ \Delta\theta_{3b} &= \Delta\theta_{1b}\sqrt{\frac{\beta_1}{\beta_3}}\frac{\sin(\psi_2-\psi_1)}{\sin(\psi_3-\psi_2)}. \end{aligned} \tag{A.11}$$

By subtracting the angular deflections of the second three-bump from the first three-bump, the undesired phase or orbit distortion introduced by the first three-bump is eliminated. The final four-bump angular deflections are expressed as

$$\begin{aligned} \Delta\theta_0 &= \Delta\theta_{0a}, \\ \Delta\theta_1 &= \Delta\theta_{1a} - \Delta\theta_{1b}, \\ \Delta\theta_2 &= \Delta\theta_{2a} - \Delta\theta_{2b}, \\ \Delta\theta_3 &= -\Delta\theta_{3b}, \end{aligned} \tag{A.12}$$

where $\Delta\theta_a$ and $\Delta\theta_b$ are listed in Equations A.8 and A.11, respectively.

Since the bump elements in this case are separators, a conversion from the μrad settings calculated above to kV settings is necessary. The kV to μrad conversion is given by

$$V[kV] = \frac{\Delta\theta[\mu rad] * p[GeV/c] * g[cm]}{l[cm] * n_{modules}}, \tag{A.13}$$

where V is the voltage across opposing separator plates and p is the momentum of the beam. The gap across the plates is denoted as g. The length of the plate is l and the number of modules which compose one separator is $n_{modules}$. In the Tevatron, the separator gap is 5 cm. A module length is 257 cm. The number of modules at each location is shown in Figure 5.1.

Separator Lattice Parameters

Location	F17	A17	A49	B11	B17	B17	C49	D11
# horizontal modules	1	0	1	2	4	0	1	2
# vertical modules	0	1	2	1	0	4	2	1
β_x (m)	52.9	-	832.8	298.4	68.1	-	774.2	278.6
β_y (m)	-	40.8	251.2	711.8	-	26.8	247.7	686.7
ψ_x (rads)	24.5	-	60.2	63.3	68.9	-	104.6	107.8
ψ_y (rads)	-	44.5	61.9	65.0	-	89.1	106.3	109.4

Table A.1: Separator lattice parameters in Collider Run IA. A phase advance of zero is defined at the E0 straight section. Lattice values are averaged over the number of modules.

Table A.1 lists the lattice functions of the separators in Collider Run IA. The lattice functions listed are values averaged over the number of modules.

Appendix B

Luminosity as a Function of Separation and Crossing Angle

This appendix presents a calculation of luminosity as a function of transverse separation and crossing angle of two colliding particle distributions. It closely follows the luminosity calculation for head-on collisions as described by Month.[63] Note that this is an alternative derivation of luminosity as compared with Equation 1.1, which is a definition of luminosity.

The luminosity, L, is a relativistic invariant. It is described by

$$L = c\sqrt{|\,\vec{\beta}_1 - \vec{\beta}_2\,|^2 - |\,\vec{\beta}_1 \times \vec{\beta}_2\,|^2}\; I(x,y,z,t) \tag{B.1}$$

where the parameter c is the speed of light and $\vec{\beta}$ is the particle velocities in units of the speed of light. The subscripts 1 and 2 denote bunches 1 and 2, respectively. The overlap integral, $I(x,y,z,t)$, is the overlap of the colliding particle distributions integrated over three-dimensional space and time.

$$I(x,y,z,t) = \int_{-\infty}^{\infty} dV \int_{-\infty}^{\infty} dt\; \rho_1(x,y,z,t)\,\rho_2(x,y,z,t) \tag{B.2}$$

where $dV \equiv dx\,dy\,dz$ represents an integration over space and t represents an integration over time.

The particle distributions, assumed Gaussian, colliding with a transverse separation of magnitude d_x and d_y in the horizontal and vertical planes, respectively, are given by

$$\rho_1(x,y,z,t) = \frac{N_1}{(2\pi)^{3/2}\sigma_{1x}\sigma_{1y}\sigma_{1z}} \exp\left(-\frac{1}{2}\left[\frac{x^2}{\sigma_{1x}^2} + \frac{y^2}{\sigma_{1y}^2} + \frac{(z-\delta_1)^2}{\sigma_{1z}^2}\right]\right) \tag{B.3}$$

$$\rho_2(x,y,z,t) = \frac{N_2}{(2\pi)^{3/2}\sigma_{2x}\sigma_{2y}\sigma_{2z}} \exp\left(-\frac{1}{2}\left[\frac{(x-d_x)^2}{\sigma_{2x}^2} + \frac{(y-d_y)^2}{\sigma_{2y}^2} + \frac{(z-\delta_2)^2}{\sigma_{2z}^2}\right]\right). \tag{B.4}$$

The number of particles per bunch is given by N. The longitudinal offset of the centroids of the colliding bunches is given by δ. If one of the bunches, for example, is centered at the collison point at $t = 0$ and the other bunch is offset from the collision point by an amount z_0 at $t = 0$, the longitudinal offset parameters satisfy $\delta_1 = ct$ and $\delta_2 = -ct + z_0$. The rms bunch size is parameterized by σ in both the transverse and longitudinal planes.

Recall from Equation 2.28 that σ is itself a function of z:

$$\sigma(z) = \sqrt{\beta(z)\epsilon + \left(\eta(z)\frac{\sigma_p}{p}\right)^2}, \tag{B.5}$$

where $\beta(z)$ is described by Equation 2.44 and the dispersion $\eta(z)$ is linear through a drift space: $\eta(z) = \eta_{z=0} + \eta' z$. In terms of accelerator parameters, the rms momentum spread of a bunch is given by[66]

$$\left(\frac{\sigma_p}{p}\right) = \frac{1}{\beta_{rel}}\sqrt{\frac{2(eV)}{\pi h \mid \eta \mid E_s}}\sin\left(\frac{\sigma_z h}{2R}\right). \tag{B.6}$$

The peak accelerating voltage per turn is given by (eV). Relativistic beta is explicitely written as β_{rel}. The harmonic number is denoted by h. The radius of the accelerating ring is given by R and the total synchronous energy is E_s. The frequency dispersion parameter, η, is dependent upon both the transition gamma, γ_t, and relativistic gamma, γ_{rel}:

$$\eta = \left|\frac{1}{\gamma_t^2} - \frac{1}{\gamma_{rel}^2}\right|. \tag{B.7}$$

The instantaneous luminosity, $L(t)$, is in units of $cm^{-2}\,sec^{-1}$. The luminosity per bunch collision, $\mathcal{L}$, is found by integrating over time and is in units of cm^{-2}.

The integration of the overlap integral over transverse space is solved analytically:

$$\int_{-\infty}^{\infty} dk\, \exp\left(-\frac{1}{2}\left[\frac{k^2}{\sigma_{1k}^2} + \frac{(k-d_k)^2}{\sigma_{1k}^2}\right]\right) = \sqrt{\frac{2\pi\sigma_{1k}^2\sigma_{1k}^2}{(\sigma_{1k}^2+\sigma_{2k}^2)}}\exp\left[\frac{-d_k^2}{(\sigma_{1k}^2+\sigma_{2k}^2)}\right] \tag{B.8}$$

where $k \equiv x, y$ represents either transverse dimension.

The integral over time is also analytically solved:

$$\int_{-\infty}^{\infty} dt\, \exp\left(-\frac{1}{2}\left[\frac{(z-ct)^2}{\sigma_{1z}^2} + \frac{(z+ct-z_0)^2}{\sigma_{2z}^2}\right]\right) = \frac{1}{c}\sqrt{\frac{2\pi\sigma_{1z}^2\sigma_{2z}^2}{(\sigma_{1z}^2+\sigma_{2z}^2)}}\exp\left[\frac{(2z-z_0)^2}{(\sigma_{1z}^2+\sigma_{2z}^2)}\right] \tag{B.9}$$

For convenience, define the new parameters:

$$\begin{aligned} \sigma_x^2(z) &= \sigma_{1x}^2(z) + \sigma_{2x}^2(z), \\ \sigma_y^2(z) &= \sigma_{1y}^2(z) + \sigma_{2y}^2(z), \\ \sigma_z^2 &= \sigma_{1z}^2 + \sigma_{2z}^2. \end{aligned} \tag{B.10}$$

Upon combining the results of the integrations of Equations B.8 and B.9, the overlap integral becomes a function of longitudinal space only.

$$I = \frac{N_1 N_2}{(2\pi)^{3/2}\sigma_z\, c} \int_{-\infty}^{\infty} dz \frac{1}{\sigma_x(z)\,\sigma_y(z)} \exp\left[-\frac{d_x^2}{2\sigma_x^2(z)} - \frac{d_y^2}{2\sigma_y^2(z)} - \frac{(2z-z_0)^2}{2\sigma_z^2}\right] \tag{B.11}$$

At high energy, the relativistic factor of Equation B.1 for two colliding bunches is very nearly equal to 2, since $|\,\vec{\beta}_1 - \vec{\beta}_2\,| \simeq 2$ and $|\,\vec{\beta}_1 \times \vec{\beta}_2\,| \simeq 0$. Thus the luminosity per bunch crossing is given by

$$\mathcal{L} = \frac{N_1 N_2}{(2\pi)^{3/2}\sigma_z\, c} \int_{-\infty}^{\infty} dz \frac{1}{\sigma_x(z)\,\sigma_y(z)} \exp\left[-\frac{d_x^2}{2\sigma_x^2(z)} - \frac{d_y^2}{2\sigma_y^2(z)} - \frac{(2z-z_0)^2}{2\sigma_z^2}\right], \tag{B.12}$$

where only one numerical integration remains.

By making an assumption that the transverse beam size is independent of z, the above expression for the luminosity is analytically expressed as

$$\mathcal{L}(\sigma \neq \sigma(z)) = \frac{N_1 N_2}{2\pi\sigma_x\sigma_y} \exp\left[-\frac{d_x^2}{2\sigma_x^2} - \frac{d_y^2}{2\sigma_y^2}\right]. \tag{B.13}$$

If there is no beam separation and a round beam assumption is made such that $\sigma_{1x} = \sigma_{2x} = \sigma_{1y} = \sigma_{2y} = \sigma$, the familiar expression for the luminosity is obtained:

$$\mathcal{L} = \frac{N_1 N_2}{4\pi\sigma^2}. \tag{B.14}$$

If a crossing angle is present, the transverse separation d is replaced by

$$d_i = d_{i_0} + 2z \tan\frac{\alpha_i}{2}, \tag{B.15}$$

where the subscript $i \equiv x, y$ denotes a transverse plane. The existence of a beam separation is included in the term d_0. The crossing angle α is the full crossing angle as depicted in Figure B.1. Upon substituting the above expression into Equation B.12 and making the assumption that transverse sigma are independent of z, one obtains a luminosity expression

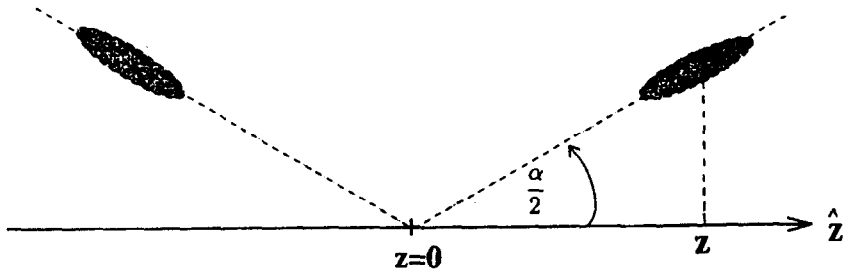

Figure B.1: A schematic of two bunches colliding with a full crossing angle α.

dependent upon a crossing angle. For a crossing angle in the horizontal plane, the luminosity is

$$\mathcal{L} = \frac{N_1 N_2}{2\pi\sigma_y\sigma_{xz}}, \tag{B.16}$$

where $\sigma_{xz} = \sqrt{\sigma_x^2 + \sigma_z^2 \tan^2\frac{\alpha_x}{2}}$. This expression assumes that $d_0 = 0$ in both transverse planes and that $z_0 = 0$. If a round beam is assumed, the familiar dependence of luminosity on a crossing angle in one dimension is obtained:

$$\mathcal{L} = \frac{N_1 N_2}{2\pi\sigma_i^2\sqrt{1 + \frac{\sigma_z^2}{\sigma_i^2}\tan^2\frac{\alpha_i}{2}}}, \tag{B.17}$$

where the subscript $i \equiv x, y$ denotes a given transverse plane.[15]

Appendix C

A Historical Review of the Use of Electrostatic Separators in Colliders [1]

Coinciding with efforts to reduce observed luminosity limitations, electrostatic separators were used at a very early stage in the development of colliders.

Beam-beam interaction effects were observed to be a luminosity limitation in the VEPP-2 electron-positron collider in Novosibirsk in 1965. "Effects of electromagnetic interaction between colliding beams ('Beam-beam phenomena') seem to place rather principle restrictions on the achievable luminosity."[69] Beam-beam luminosity limitations seem to have led quite naturally to an implementation of electrostatic separators in colliders in order to separate particles of opposite charge in the same storage ring and decrease beam-beam interaction effects.

There were several early uses of electrostatic separators in a variety of storage rings. The VEPP-2 storage ring was colliding electrons and positrons in 1967 at a center-of-mass energy of 400 MeV. An "orbit splitting" technique with the help of an electric field was used at that time. Beam separation enabled stored electrons to reach currents of 100 mA without large positron losses.[1] Two years later, the Orsay collaboration in France was also faced with a beam-beam luminosity limitation in the ACO electron-positron collider. A current limit of 20 mA per bunch existed for two colliding bunches at a center of mass energy of 1070 MeV. In order to "fight the effect", electrostatic separation was used.[70] The collider at Laboratori Nazionali di Frascati (ADONE), colliding electrons and positrons at a center-of-mass energy of 3.0 GeV, used separators for beam stability at injection.[71]

[1] This appendix is not part of the dissertation submitted to the University of New Mexico. It is included only in the Fermilab internal note.

The Cambridge Electron Facility (CEA) extended the use of separators for multibunch operation.[72] Electron and positron bunches were accelerated in the CEA in 1969 to energies of approximately 4 GeV. The bunches filled approximately one-third of the synchrotron. Vertical separation was used to separate bunches at parasitic crossing points.[73] "Physical separation with electrostatic fields....is necessary to avoid short lifetimes of the weaker of the two beams due to the incoherent space charge interaction."[74] Separated orbits of the electrons and positrons in the storage ring were kicked onto the same closed orbit in the bypass interaction region and collided head-on at the interaction region.[75]

Electrostatic separators continued to be utilized as higher energy electron-positron colliders were constructed, such as the 6.0 GeV (center-of-mass) SPEAR electron-positron collider at Stanford Linear Accelerator Complex (SLAC).[76]

A major technical difficulty in operation of electrostatic separators is in maintaining a spark rate of zero. One spark often proves disasterous for a colliding beam store. The first electrostatic separators operated at voltages of approximately 10 kV/cm. As particles were accelerated to higher energies, voltage requirements on electrostatic separators increased to approximately 50 kV/cm. These high voltage separators were built almost simultaneously and independantly for the SPS proton-antiproton collider at CERN and for the CESR electron-positron collider at Cornell University. Both accelerator collaborations presented experimental results on their newly deviced "pretzel orbit schemes" at the 1985 IEEE Particle Accelerator Conference (Vancouver) with no reference to each other![77],[78] CESR began using electrostatic separators in the horizontal plane to allow for multi-bunch operation and raise the luminosity.[79] The SPS implemented a horizontal orbit separation in order to decrease the beam-beam tune shift of the antiprotons and accomodate collisions of six antiproton and six proton bunches.[80]

Electrostatic separators remain an integral part of many high-energy colliders which were constructed in recent years. The Tevatron Collider at Fermilab collides protons and antiprotons at a center of mass energy of 1800 GeV. The Collider had reached a luminosity limit due to the beam-beam interaction in its first Collider Run in 1988. One could not increase the luminosity by decreasing the transverse size of the proton bunch or by increasing the number of protons per bunch. In fact, it was necessary to dilute phase space density of the protons in order to maintain stability of the antiprotons.[81] Taking advantage of the equal transverse size of the bunch distributions (round beams), the Tevatron implemented a helical orbit scheme by separating the orbits of the protons and antiprotons in both the horizontal and vertical planes. The opposing particle distributions are separated everywhere

in the ring except at the locations of the two high energy physics detectors.[82] The achievable luminosity of $1.6 \times 10^{30}\text{cm}^{-2}\text{sec}^{-1}$ without beam separation increased to luminosities of $5.4 \times 10^{30}\text{cm}^{-2}\text{sec}^{-1}$ in routine operations with helical orbits in the following Collider Run.[3]

In CERN's electron-positron collider at LEP, consideration of different operational configurations of electrostatic separators has continually led to increases in the luminosity. In 1990, the LEP ring began to collide four bunches of electrons and positrons at a center-of-mass energy of 90 GeV at four high energy physics detector locations. Vertical separators were used to separate the beam at the four parasitic locations in the accelerating ring. Following the multi-bunch scheme developed at CESR, more separators were installed at LEP and more bunches were accelerated (up to eight) shortly afterwards.[83],[84] To further increase the luminosity, a recent proposal for a "bunch-train" scheme has been approved which consists of accelerating four equidistant trains of bunches in each beam instead of four to eight single bunches.[85] Previous problems with sparking of electrostatic separators in LEP have been essentially eliminated by always operating one electrostatic plate at ground potential and the other at positive potential.[86]

Plans for future accelerators continue to include electrostatic separators as a tool in avoiding luminosity limitations due to the beam-beam interaction. Recent studies of expected beam-beam effects in CERN's Large Hadron Collider (LHC) have determined that the main limit to the luminosity will be the beam-beam effect.[87] Planned operation with closely spaced bunches in an interaction region add another level of complexity to beam-beam luminosity limitations as long-range beam-beam effects become much more significant.[88]

Bibliography

[1] V.L.Auslander, et.al., *Experimental Investigations of Beam-Beam Interaction in Storage Rings*, Proceedings of the 6th International Conference on Particle Accelerators, pp. 126-129, (1967).

[2] Dugan, G. *Tevatron Status*, Proceedings of the 1989 IEEE Particle Accelerator Conference, pp. 427-428, (1989).

[3] Private communication with Steve Holmes, Fermilab, August (1994).

[4] E.D. Courant and H.S. Snyder, *Theory of the Alternate Gradient Synchrotron*, Annals of Physics, Vol. 3, pp. 1-48, (1958).

[5] Fermi National Accelerator Laboratory, *Design Report - Tevatron 1 Project*, September (1984).

[6] F.T.Cole and R. Donaldson, *Proceedings of the 12th International Conference on High Energy Accelerators*, Fermilab National Accelerator Laboratory, August (1983).

[7] F.T.Cole, R. Donaldson et. al., *A Report on the Design of the Fermi National Accelerator Laboratory Superconducting Accelerator* ,Fermilab National Accelerator Laboratory, May (1979).

[8] G. Floquet, Ann. Ecole Normale (2) 12 (1883) 47.

[9] D.A.Edwards and M.J.Syphers, *An Introduction to the Physics of High Energy Accelerators*, Wiley Series in Beam Physics and Accelerator Technology, (1993).

[10] S. Holmes, *A Practical Guide to Modern High Energy Accelerators*, Fermilab-Conf-87/160, October (1987).

[11] E. Wilson, *Transverse Beam Dynamics*, Proceedings of the CERN Accelerator School in General Accelerator Physics, CERN 85-19, pp. 64-95, (1984).

[12] E. Wilson, *Proton Synchrotron Accelerator Theory*, CERN 77-07, March (1984).

[13] W.G. Clark, *Introduction to Magnetic Resonance and its Application to Dipole Magnet Testing*, CERN Accelerator School on Magnetic Measurement and Misalignment, March (1992).

[14] Satogata, T. *Nonlinear Resonance Islands and Modulational Effects in a Proton Synchrotron*, Dissertation, Northwestern University (1993).

[15] Sands, M. *The Physics of Electron Storage Rings: An Introduction*, SLAC-121, November (1970).

[16] Ohnuma, S. *The Beam Emittance*, EXP-111, November (1983).

[17] Based on calculations done by Norman Gelfand, Fermilab, February (1993).

[18] Calculations were based on a Tevatron model *Tevconfig* developed by Glenn Goderre, Fermilab.

[19] Calculations and plots done by Glenn Goderre, Fermilab, October (1994).

[20] Private communication with Glenn Goderre, Fermilab, October (1994).

[21] L. Michelotti, *Intermediate Classical Dynamics*, John-Wiley Press, (1995).

[22] A.W.Chao, *Nonlinear Beam-Beam Resonances*, Joint US/CERN School on Particle Accelerators, Italy, SLAC-PUB-3545, January (1985).

[23] L.R. Evans,*The Beam-Beam Interaction*, CERN SPS/83- 38 (DI-MST) (1983).

[24] S.G. Peggs and R.M. Talman, *Nonlinear Problems in Accelerator Physics*, Ann. Rev. Nucl. Part. Sci., 36, p. 287 (1986).

[25] K. Cornelius, M. Meddahi, R. Schmidt, *Experiments on the Beam-Beam effect in the CERN-SPS 1989 collider run*, SPS/AMS/Note 89-13.

[26] K. Cornelius, M. Meddahi, R. Schmidt, *The beam-beam effect in the SPS proton antiproton collider for beams with unequal emittances*, CERN SL/90-73 (AP).

[27] S. Saritepe, L. Michelotti, S. Peggs, *Long-Range Beam-Beam Interactions in the Tevatron: Comparing Simulation to Tune Shift Data*, FERMILAB-Conf-90/134.

[28] Bambade, Ph. D. thesis, *Effets faisceau-faisceau dans les anneaux de stockage e+ e- á haute énergie: grossissement résonant des dimensions verticales dans le cas de faisceaux plats.*, LAL84/21, June 1984, Universite de Paris Sud, Centre d'Orsay.

[29] Meddahi, M., Ph. D. thesis, *Effets faisceau-faisceau dans le Collisionneur Protons-Antiprotons du SPS*, CERN SL/91-30(BI), July 1991, Universite de Paris Sud, Centre d'Orsay.

[30] Goldstein, H., *Classical Mechanics*, Addison-Wesley (1980).

[31] Ruth, R., *Single Particle Dynamics and Nonlinear Resonances in a Circular Accelerator*, Lecture Notes in Physics No. 247: Proceedings of the Joint US-CERN School on Particle Accelerators, Springer-Verlag (1985).

[32] L.R. Evans and J. Gareyte,*Beam-Beam Effects*, CERN Accelerator School, Sept. 1985, CERN 87-03, Vol. I, p. 159.

[33] A.W.Chao, *Nonlinear Dynamics and the Beam-Beam Interaction*, AIP Conference Proceedings, No. 57. pg. 42-68 (1979).

[34] Herr, W., *Tune Shifts and Spreads Due to Short and Long Range Beam-Beam Interactions in the LHC*, CERN SL/90-06, March (1990).

[35] Herr, W., *Tracking studies on the beam-beam effect in the Cern - SPS p pbar Collider*, CERN SL/91-05 (AP), September (1991).

[36] Private communication with Werner Herr, CERN, October (1994).

[37] Myers, S., *Nonlinear Dynamics Aspects of Particle Accelerators*, Lecture Notes in Physics No. 247: Proceedings of the Joint US-CERN School on Particle Accelerators, Springer-Verlag (1985), pp. 176-237.

[38] Bassetti, M. and Erskine, G., CERN ISR-TH/80-06, March (1980).

[39] Y. Okamoto and R. Talman, *Rational Approximation of the Complex Error Function and the Electric Field of a Two-Dimensional Gaussian Charge Distribution*, CBN80-13, September (1980).

[40] S. Saritepe, G. Goderre, S. Peggs, *Observations of the Beam-Beam Interaction in Hadron Colliders*, FERMILAB-FN-573 (1991).

[41] S. Peggs, *Hamiltonian Theory of the E778 Nonlinear Dynamics Experiment*, SSC-175, April (1988).

[42] S. Peggs, *Iteration and Accelerator Dynamics*, SSC-144, October 1987.

[43] S. Peggs, *Hadron Collider Behaviour in the Nonlinear Numerical Model EVOL*, Particle Accelerators, Vol. 17, p:11-50 (1987).

[44] Private communication with Werner Herr, CERN, February (1995).

[45] R. Siemann, *Summary of Measurements of Betatron Line Amplitudes, RF Phase Noise and Emittance Growth*, Fermilab Internal Experimental Note, EXP-155, August (1987).

[46] D. Boussard, *Schottky Noise and Beam Transfer Diagnostics*, Proceedings of the CERN Accelerator School for General Accelerator Physics, CERN 87-03 (1987).

[47] G. Jackson, *Tune Spectra in the Tevatron Collider*, Proceedings of the IEEE Particle Accelerator Conference, pp. 860-862 (1989).

[48] D. Martin, et al, *A Resonant Beam Detector for Tevatron Tune Monitoring*, Proceedings of the IEEE Particle Accelerator Conference, pp. 1486-1488 (1989).

[49] Figures 4.2 and 4.3 contributed by Milciades Contreras, University of Chicago collaboration at CDF.

[50] C. Grosso-Pilcher and S. White, *CDF Luminosity Calibration*, Fermilab Note FN-550, October (1990).

[51] P. Michals, *Precision in SBD Measurement*, Fermilab Internal Experimental Note, Fermilab Note, EXP-163, March (1989).

[52] Measurement and plot done by E. Barsotti, Fermilab, October (1994).

[53] E. Barsotti, *The Sampled Bunch Display (SBD) Upgrade*, Fermilab Operations Bulletin, no. 1257, March (1994).

[54] Private communication with Ed Barsotti, Fermilab, July (1994).

[55] J. Gannon, et al, *Flying Wires at Fermilab*, Proceedings of the IEEE Particle Accelerator Conference, pp. 68-70 (1989).

[56] J. Zagel, et al, *Upgrades to the Fermilab Flying Wire Systems*, Proceedings of the IEEE Particle Accelerator Conference, pp. 1174-1176 (1991).

[57] Private communication with Glenn Goderre, Fermilab, February (1995).

[58] Private communication with Greg Vogel, Fermilab, July (1994).

[59] W.C. Carithers et al, *The CDF SVX: A Silicon Vertex Detector for a Hadron Collider*, Nuclear Instruments and Methods in Physics Research A289, pp. 388-399 (1990).

[60] Private communication with Mike Martens, Fermilab, March (1995).

[61] R. Dubois, et al, *Beam Separation Experiments at the SPS Collider*, CERN SPS/85-5, January (1985).

[62] S. van der Meer, *Calibration of the Effective Beam Height in the ISR*, ISR-PO/68-31, June (1968).

[63] M. Month, *Collider Performance with Ideal Collisions*, Internal Fermilab D0 Note 201, (1985).

[64] Calculations and plots using SVX data were done by Paul Derwent, University of Michigan collaboration at CDF, December (1994).

[65] Private communication with R. Schmidt, K. Cornelius, M. Meddahi and W. Herr of CERN, February (1994).

[66] S. Ohnuma, *The Beam and the Bucket*, Fermilab Internal Note TM-1381, (1986).

[67] B. Hanna, *Turning on the Separators*, Fermilab Operations Bulletin 1207, November (1990).

[68] H. Grote and C. Iselin, *The MAD Program*, CERN/SL/90-13, rev. 3, January (1993).

[69] V.L. Auslander, et.al., *Experimental Results on Beam-beam Interaction*, Proceedings of the 5th International Conference on Particle Accelerators, pp. 335-339, (1965).

[70] J.E. Augustin, et. al., *Development and Beam Studies on ACO*, Proceedings of the 7th International Conference on Particle Accelerators, pp. 19-24, (1969).

[71] F. Amman, et. al., *Single and Two Beam Operation in Adone*, Proceedings of the 7th International Conference on Particle Accelerators, pp. 9-18, (1969).

[72] A. Hofmann, et. al., *The Colliding Beam Project at the Cambridge Electron Accelerator*, Proc. of the Sixth International Conference on High Energy Accelelerators, pp. 113-118, (1967).

[73] T. Dickinson, *Electrostatic Separation of Stored Beams at CEA*, IEEE Transactions on Nuclear Science, pp. 196-198, (1971).

[74] R. Averill, et. al., *Colliding Electron and Positron Beams in the CEA Bypass*, Proc. of the Eighth International Conference on High-Energy Accelerators, pp. 140-144, (1971).

[75] C. Mieras and G.A. Voss, *A Design of the CEA Colliding Beam Bypass*, Proc. of the Sixth International Conference on High Energy Accelelerators, pp. 119-122, (1967).

[76] B. Richter, *Colliding Beams: Present Status; and the SLAC Project*, IEEE Transactions on Nuclear Science, Vol. NS-18, No. 3, pp. 193-195, June (1971).

[77] R. Littauer, *Multibunch Operation of CESR*, Proceedings of the IEEE Transactions on Nuclear SCience, Vol. NS-32, No. 5, pp 1610-1613, October (1985).

[78] L. Evans, et.al., *Beam Separation at the CERN SPS Collider*, Proceedings of the IEEE Transactions on Nuclear SCience, Vol. NS-32, No. 5, pp 2209-2211, October (1985).

[79] S. Herb, CESR: Projects and Prospects, Proceedings of the 13th International Conference On High Energy Accelerators, pp. 58-62, August (1986).

[80] K. Cornelis, *Beam-beam Effects and High Luminosity Operation in the SPS Proton Antiproton Collider*, CERN SPS/86-14, September (1994).

[81] S.D. Holmes, *The Fermilab Upgrade*, Proceedings of the IEEE Particle Accelerator Conference, pp. 436-438, March (1989).

[82] G. Annala, *Operational Experience with the Tevatron Collider using Separated Orbits*, Proceedings of the IEEE Particle Accelerator Conference, pp. 3808-3810, May (1993).

[83] J.M. Jowett, *More Bunches in LEP*, CERN LEP-TH/89-17, Proceedings of the IEEE Particle Accelerator Conference (Chicago, IL), p.1806, March (1989).

[84] Cern Courier: International Journal of High Energy Physics, *The Best of the Bunch*, Edited by G. Frasier, pp. 18-20, October (1992).

[85] C. Bovet, et.al., *Final Report of the 1994 Bunch Train Study Group*, CERN SL/94-95-(AP), December (1994).

[86] E. Keil, *Review of High Energy e^+e^- Colliders*, Proceedings of the European Particle Accelerator Conference EPAC92 (Berlin, Germany), pg. 22-26, March (1992).

[87] W. Herr, *Beam-beam Effects in the LHC*, CERN SL/94-92-(AP), November (1994).

[88] W. Herr, *Tune Shifts and Spreads due to Long Range Beam-beam Effects in the LHC*, CERN SL/90-06-(AP), March (1990).